International Journal of Mass Spectrometry 305 (2011) 199–208

Contents lists available at ScienceDirect

International Journal of Mass Spectrometry

journal homepage: www.elsevier.com/locate/ijms

Fragmentation of neutral oligosaccharides using the MALDI LTQ Orbitrap

Marion Rohmer[a], Dominic Baeumlisberger[a], Bernd Stahl[b], Ute Bahr[a], Michael Karas[a,*]

[a] Institute of Pharmaceutical Chemistry, Goethe-University Frankfurt, Max-von-Laue-Strasse 9, 60438 Frankfurt am Main, Germany
[b] Danone Research Centre for Specialised Nutrition, Bahnstrasse 14-30, 61381 Friedrichsdorf, Germany

ARTICLE INFO

Article history:
Received 28 July 2010
Received in revised form 4 November 2010
Accepted 8 November 2010
Available online 17 November 2010

Keywords:
MALDI
Derivatization
Orbitrap
Fragmentation
Structural analysis
Human milk oligosaccharide

ABSTRACT

Matrix-assisted laser desorption/ionization time-of-flight mass spectrometry is a highly appreciated method in oligosaccharide analysis due to its high sensitivity and ease of use. As underivatized oligosaccharides suffer from low ionization efficiency, derivatization is a widespread tool. However, subsequent sample purification and toxic or otherwise dangerous reagents complicate the oligosaccharides' analysis. On-target derivatization performed by the matrix 3-aminoquinoline does not require such purification and yields Schiff bases which can be measured in positive and negative ion modes from one single spot. In this article, this simple and convenient method is applied for structural characterization of oligosaccharides using a MALDI LTQ Orbitrap. Information received by the different fragmentation techniques collision-induced dissociation (CID), pulsed-Q dissociation (PQD) and higher energy C-trap dissociation (HCD) are compared. By combining the information received from fragmentation of $[M+H]^+$ ions (in positive ion mode) and $[M+NO_3]^-$ ions (in negative ion mode) of 3-AQ-derivatized species by all three fragmentation techniques, a complete structural characterization in terms of linkage, branching and anomeric configuration of glycosidic bonds of oligosaccharides could be achieved. The analysis of isomeric human milk oligosaccharides derivatized with 3-AQ yielded comprehensive information on the isomers' structures. Finally, a simple combination of peak lists obtained by the different fragmentation techniques and automatic measurements enhance and facilitate oligosaccharide analysis.

1. Introduction

Mass spectrometry (MS) has clearly established itself in oligosaccharide analysis during recent years [1–8]. However, the high complexity of oligosaccharides due to differences in sequence, linkage position, branching and anomeric configuration of glycosidic bonds make their structural analysis by mass spectrometric measurements challenging [9] and fragmentation an essential tool, especially for the distinction of isobaric structures.

Fragmentation of oligosaccharides has been examined to a great extent by infrared laser desorption [10], fast atom bombardment (FAB) [11], electrospray ionization (ESI) [5,12–14] and matrix-assisted laser desorption/ionization (MALDI) [2,4,6,15,16] MS. For structural characterization of oligosaccharides, electrospray ionization followed by collision-induced dissociation in ion traps is the method of choice due to superior ionization and fragmentation characteristics [7]. Oligosaccharide analysis using MALDI ion sources, which were usually combined with time-of-flight (TOF) mass analyzers in the past, was therefore restricted to in-source decay (ISD) and post-source decay (PSD) fragmentation [1,17]. MALDI-ISD mainly produces fragments which are identical to molecular ions of other oligosaccharide species, complicating the analysis of oligosaccharide mixtures [17]. MALDI-PSD fragmentation, yielding fragment ions detected in TOF/TOF instruments, suffers from low fragmentation efficiency and resolution. As PSD spectra in positive ion mode are dominated by glycosidic cleavages [16], the distinction of isomers is rather difficult. The abundance of cross-ring cleavages could be increased by the introduction of a collision cell [18,19] and resolution could be improved by orthogonal-TOF mass analyzers [20]. But only the combination of a MALDI ion source and a Q-TOF mass analyzer yields high-quality CID spectra which are comparable to the respective electrospray-ionized ones, but yet less complicated due to the absence of multiply charged ions [21].

Both MALDI and ESI as ionization techniques are used in positive as well as negative ion mode, as only a combination of both modes provides complete information on the oligosaccharide's structure in terms of sequence, linkage, branching and anomeric configura-

Abbreviations: MALDI, matrix-assisted laser desorption/ionization; ESI, electrospray ionization; 3-AQ, 3-aminoquinoline; CID, collision-induced dissociation; PQD, pulsed-Q dissociation; HCD, higher energy C-trap dissociation; PSD, post-source decay; TOF, time-of-flight; FWHM, full width at half maximum; CFG, Consortium for Functional Glycomics; HMOS, human milk oligosaccharides; TFLNH, trifucosyllacto-*N*-hexaose; TFpLNH, trifucosyl-para-lacto-*N*-hexaose.

* Corresponding author. Tel.: +49 0 69 798 29916; fax: +49 0 69 798 29918.
E-mail addresses: rohmer@pharmchem.uni-frankfurt.de (M. Rohmer), baeumlisberger@pharmchem.uni-frankfurt.de (D. Baeumlisberger), bernd.stahl@danone.com (B. Stahl), bahr@pharmchem.uni-frankfurt.de (U. Bahr), karas@pharmchem.uni-frankfurt.de (M. Karas).

1387-3806/$ – see front matter © 2010 Elsevier B.V. All rights reserved.
doi:10.1016/j.ijms.2010.11.008

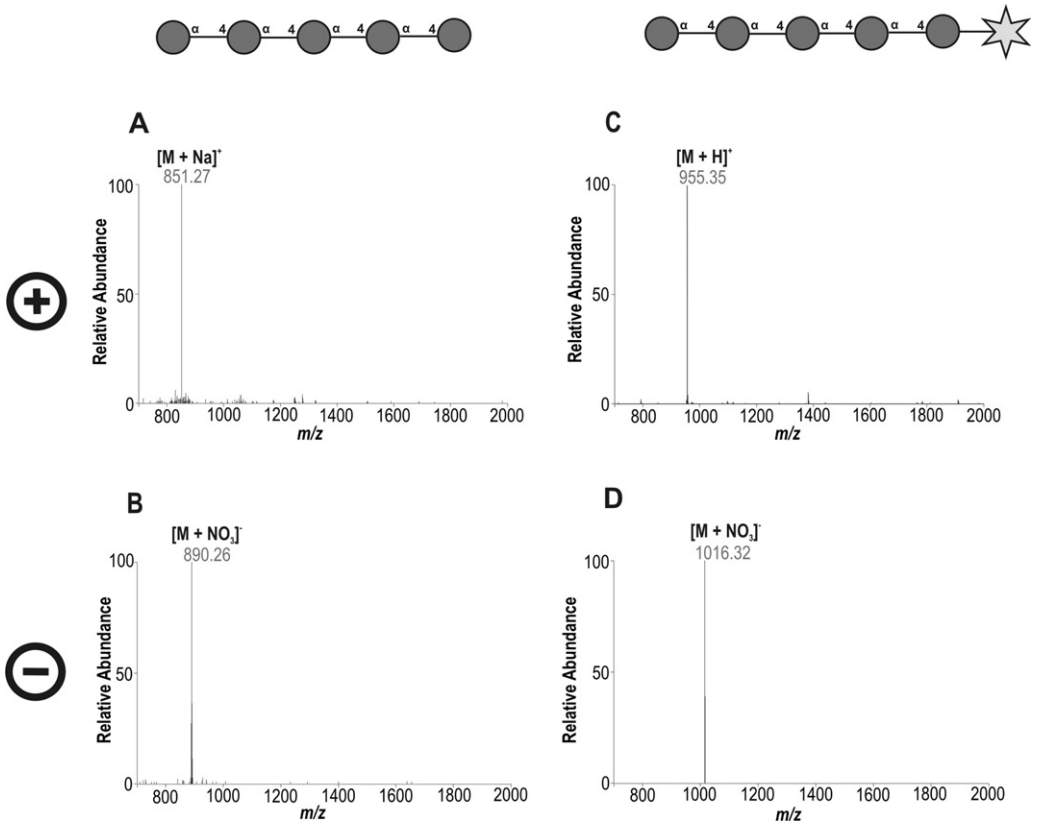

Fig. 1. MALDI MS spectra of maltopentaose with harmine (left side) or 3-AQ (right side) as matrices in positive and negative ion modes. Ionization in both modes is promoted by the addition of salts or acids. In positive ion mode, underivatized maltopentaose is ionized by sodium adduction (A), whereas introduction of the basic 3-AQ residue leads to the formation of protonated species (C). In negative ion mode, both underivatized (B) and derivatized (D) maltopentaose ionize by the addition of nitrate anions.

tion of glycosidic bonds. Information gained by fragmentation in positive and negative ion modes differs strongly [13]. In positive ion mode, underivatized oligosaccharides are ionized by adduct formation with alkali metal ions. As these cations are not localized on a fixed position of the oligosaccharide molecule [7], positive ion mode MS/MS spectra contain various types of fragment ions, most of them resulting from glycosidic bond cleavages [15,16] (B-, C-, Y-, and Z-fragments; nomenclature after Domon and Costello [22]). Positive ion mode fragmentation provides the oligosaccharide's sequence, but isomers differing in linkage positions or anomeric configurations of glycosidic bonds usually cannot be distinguished. Negative ion mode fragmentation closes this gap by yielding specific fragment ions which define linkage and branching (mostly A-ions resulting from cross-ring cleavages) [13,23,24]. As $[M-H]^-$ ions of oligosaccharides are unstable and subject to prompt fragmentation, the formation of more stable anionic adducts of oligosaccharides by the admixture of salts has been very popular in recent years [13,25]. Out of those anionic adducts, $[M+NO_3]^-$ ions are especially valuable as detection limits are low and spectra received from CID fragmentation subsequent to electrospray ionization are highly informative. However, probably due to the low gas-phase basicity of the NO_3^- ion, resulting in a high stability of $[M+NO_3]^-$ oligosaccharide ions, fragmentation of these species by post-source decay (PSD) in MALDI-TOF instruments yielded no structural information [25], and other anionic adducts with lower detection limits such as $[M+Cl]^-$ were used.

For mass spectrometric analysis of oligosaccharides, derivatization is frequently used as it enhances sensitivity and fragmentation behaviors, and is moreover compatible with a previous chromatographic separation [26]. However, adjacent sample purification steps are often associated with sample losses and complicate the derivatization procedure [27]. Recently, we described the use of 3-aminoquinoline (3-AQ) as matrix and derivatizing agent for oligosaccharide analysis [28]. Derivatization by the matrix 3-AQ is performed via formation of Schiff bases, i.e. imines, with the reducing end of oligosaccharides as illustrated in Scheme 1. Until recently, this chemical reaction was considered as undesired when using 3-AQ as matrix because it complicated spectra interpretation [6]. However, by the optimization of the preparation protocol, a quantitative and reproducible on-target derivatization was achieved [28]. Contrary to common derivatization approaches, no purification of the derivatized species is required, and the use of toxic reagents (such as sodium cyanoborohydride for reductive amination) is avoided. Ionization of the Schiff base is enhanced in positive as well as in negative ion mode, improving detection limits. First results by MALDI-TOF/TOF fragmentation of 3-AQ-derivatized oligosaccharides provided extensive information on sequence, linkage and branching.

In the following article, we describe the use of a MALDI LTQ Orbitrap for oligosaccharide analysis, providing three fragmentation techniques: collision-induced dissociation (CID), pulsed-Q dissociation (PQD) [29,30] and higher energy C-trap dissociation (HCD) [31,32]. CID, PQD and HCD fragmentation were carried out with 3-AQ-derivatized and, as a comparison, with underivatized oligosaccharides in positive and negative ion modes. Information received by all resulting spectra is gathered and the ability to distinguish isomers is examined.

2. Experimental

2.1. Materials and methods

Commercially available isomeric oligosaccharides (3α,6α-mannopentaose, maltopentaose, cellopentaose), 3-amino-

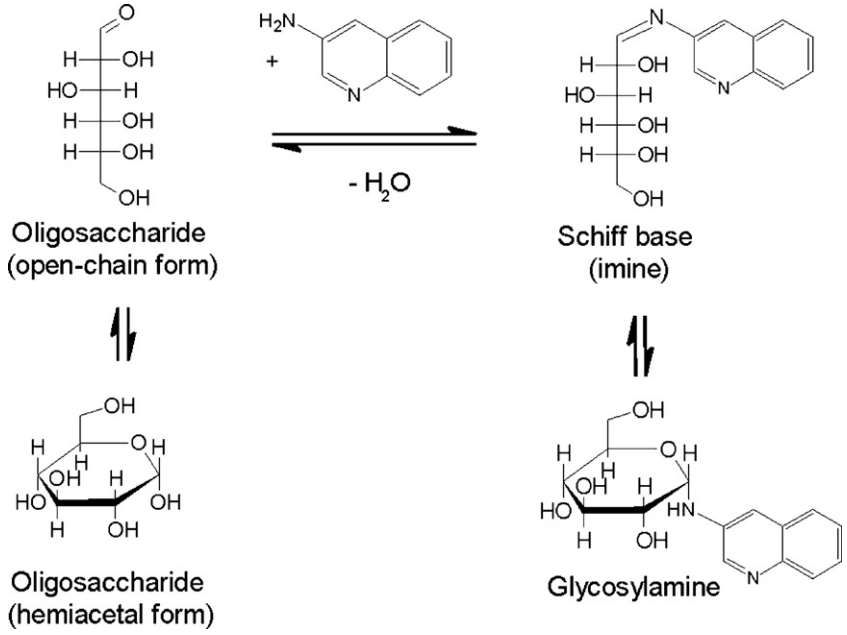

Scheme 1. Schiff base formation of reducing-end oligosaccharides with 3-AQ.

quinoline, harmine-HCl, ammonium nitrate, sodium chloride and nitric acid were purchased from Sigma (St. Louis, MO). Isomeric human milk oligosaccharides, trifucosyllacto-*N*-hexaose and trifucosyl-para-lacto-*N*-hexaose, were obtained from Danone Research Centre for Specialised Nutrition (Friedrichsdorf, Germany). All oligosaccharides were dissolved in ultrapure water produced by a Milli-Q system (Millipore, Billerica, MA). Acetonitrile (ACN, gradient grade) and ethanol were obtained from Carl Roth (Karlsruhe, Germany).

2.2. Preparation of spots

Oligosaccharide and matrix solutions (1 μL each) were mixed together on a stainless steel target. Harmine-HCl (10 mg/mL) was prepared in 80% ethanol/20% 25 mM ammonium nitrate and 25 mM sodium chloride in water. 20 mg/mL of 3-AQ were dissolved in an ACN–water mixture (1:2 v/v) and the solution's pH was adjusted to 5.5 by the addition of 0.07% nitric acid. Derivatization with 3-AQ was performed according to the optimized preparation protocol described elsewhere [28]. Briefly, the dried-droplet technique was used for preparation (optimized matrix solution see above). Complete derivatization and crystallization were achieved in approximately 2 h at ambient temperature. Neither a precedent admixture of 3-AQ as derivatizing agent nor a subsequent purification of derivatized oligosaccharides was necessary.

2.3. Mass spectrometric analysis of oligosaccharides

All MALDI MS and MS/MS spectra were recorded on a MALDI LTQ Orbitrap XL hybrid mass spectrometer (Thermo Fisher Scientific, Bremen, Germany) in positive and negative ion modes. Instrumentation of the Orbitrap mass analyzer [33,34], performance of the LTQ Orbitrap mass spectrometer [35] and the combination with a MALDI ion source [36] have already been outlined. Full scan mass spectra were recorded in the Orbitrap mass analyzer due to its high mass accuracy. The m/z range was chosen according to the individual structure of the examined oligosaccharide. Resolution was set to 30,000 at $m/z = 400$ (FWHM). For each scan, 3 microscans were recorded from one position. Automatic gain control (AGC) was used to regulate the filling status of the linear ion trap. The survey crystal positioning system (survey CPS) allowed for the random choice of shot position by automatic crystal recognition. Laser intensity was set marginally above the threshold of ionization to avoid fragmentation, depending on matrix and oligosaccharide mass (15–20 μJ). In order to acquire MS/MS spectra, the laser energy was slightly increased. CID and PQD fragments were detected in the LTQ linear ion trap due to its higher sensitivity. Wideband activation technology was enabled to enhance structural information. For HCD experiments, whose fragments can only be detected in the Orbitrap mass analyzer, resolution was set to 7500 (FWHM) to increase sensitivity. Isolation width (m/z) was set to 3. Further settings like normalized collision energy (CE), activation Q value (Q) and activation time (T) were configured depending on the fragmentation technique:

CID: CE = 50%, $Q = 0.250$, $T = 30$ ms;
PQD: CE = 30–35%, $Q = 0.700$, $T = 0.1$ ms;
HCD: CE = 30%, $Q = 0.250$, $T = 30$ ms.

Resulting spectra were interpreted manually and assisted by GlycoWorkbench software [37].

3. Results and discussion

3.1. Ionization of oligosaccharides in positive and negative ion modes

In the following, maltopentaose is used to demonstrate the influence of derivatization with 3-AQ on adduct formation. Maltopentaose is a reducing pentasaccharide consisting of five α-1,4-linked (for its structure see Fig. 1). The symbols and abbreviations used in all following figures and the oligosaccharide masses are listed in Table 1 (symbols are according to the Nomenclature Committee of the Consortium for Functional Glycomics (CFG), see http://www.functionalglycomics.org/static/consortium/Nomenclature.shtml). Underivatized oligosaccharides are ionized in positive ion mode via addition of alkali metal ions promoted by the admixture of salts (e.g. sodium chloride, see Fig. 1A). In contrast to other common matrices such as DHB (2,5-dihydroxy benzoic acid), using harmine as matrix, maltopentaose

Table 1
Symbols, abbreviations and masses of all investigated monosaccharide residues (symbols according to the Consortium for Functional Glycomics, CFG).

	CFG symbols					Others
	●	◍	○	■	△	✡
Monosaccharides	Glucose	Mannose	Galactose	*N*-Acetylglucosamine	Fucose	3-Aminoquinoline
Abbreviation	Glc	Man	Gal	GlcNAc	Fuc	3-AQ
Mass (Da)	180.1	180.1	180.1	221.1	164.1	144.1
Residual mass (Da)	162.1	162.1	162.1	203.1	146.1	126.1

can also be detected in negative ion mode as anion-attached species (see Fig. 1C). Ammonium nitrate was chosen as anionizing agent because it has been reported that $[M+NO_3]^-$ ions of oligosaccharides exhibit the highest intensities of all oligosaccharide anionic adducts in ESI MS analysis [13]. Using 3-AQ, the respective Schiff base is formed by dehydration out of any reducing oligosaccharide. The optimized 3-AQ preparation protocol allows complete conversion into 3-AQ-derivatized maltopentaose, indicated by a mass shift of 126 Da. In positive ion mode, maltopentaose can now be detected as protonated species due to the basic 3-AQ residue (Fig. 1C). In negative ion mode, 3-AQ-derivatized oligosaccharides form $[M+NO_3]^-$ ions like their underivatized counterparts (Fig. 1D). The improvement in detection limits achieved by derivatization in positive ion mode (1 pmol with DHB vs. 100 fmol with 3-AQ) and negative ion mode (100 fmol with harmine vs. 1 fmol with 3-AQ) has already been described [28].

3.2. CID, PQD and HCD fragmentation in positive and negative ion modes

The MALDI LTQ Orbitrap XL provides three fragmentation techniques as mentioned above [29–36]. Those differ in the kinetic energy applied for precursor excitation and dissociation and in the components of the LTQ Orbitrap system in which fragmentation is performed. The energy received by the precursor, which highly influences fragment generation, is expressed by *Q*-values controlled via the radio frequency amplitude. First of all, *collision-induced dissociation* (*CID*) is a standard fragmentation technique made accessible by any ion trap. Unfortunately, the constant *Q* value ($Q = 0.25$) of CID does not allow the trapping of fragments with *m*/*z* values lower than 28% of the precursor mass (so-called "one-third rule") [30]. Second, the *pulsed-Q dissociation* (*PQD*) technique, being implemented in some linear ion traps, exhibits a process divided into three steps. After activation at high *Q* values ($Q > 0.6$), the precursor is fragmented during a time delay at high *Q*. This is followed by a rapid pulse to a lower *Q* value, enabling the capture of fragments with lower *m*/*z* values. Both CID and PQD fragments can be detected in the LTQ linear ion trap as well as in the Orbitrap mass analyzer of the hybrid MALDI LTQ Orbitrap. The third technique called *higher-energy C-trap dissociation* (*HCD*) is executed in a special collision cell fitted to the C-trap device of the instrument [31,32]. Consequently, HCD fragments can only be detected in the Orbitrap mass analyzer. Both PQD and HCD have already been applied to peptide fragmentation, especially for quantification methods which rely on the generation of low-mass fragments (e.g. iTRAQ) [30,38–40]. Analysis of resulting MS/MS spectra show differences in peak intensities and mass range compared with the standard CID fragmentation, although fragment types are not significantly different [29–32,38–40]. Although PQD and HCD conducted in LTQ Orbitrap instruments should be of great benefit for oligosaccharide analysis as the additional detection of low-mass fragments should facilitate structural characterization, they have not yet been used for that purpose. Only few publications concerning HCD fragmentation of glycopeptides are available [40–42], but released glycans or other oligosaccharides have not yet been examined. Actually, oligosaccharide analysis using the MALDI LTQ Orbitrap has been described once for acidic (e.g. sialylated) oligosaccharides [43], but only CID was employed for structural characterization.

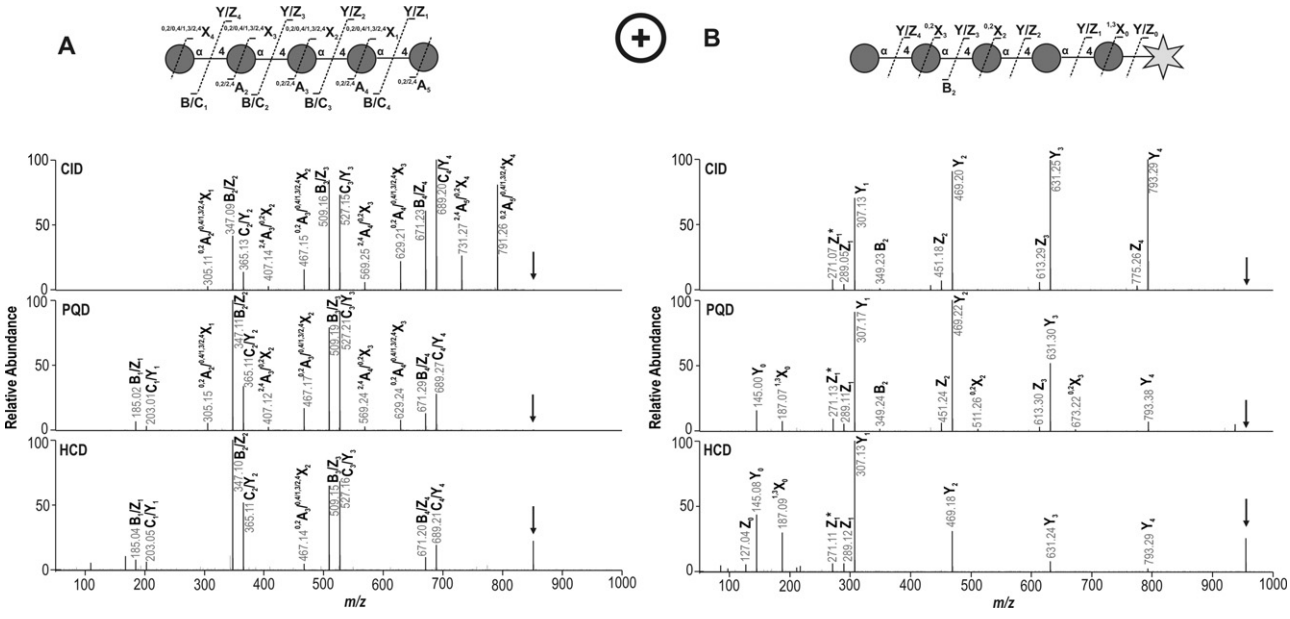

Fig. 2. Maltopentaose – spectra obtained by CID, PQD and HCD fragmentation with harmine (A)/3-AQ (B) in positive ion mode. Precursors are the respective adducts as depicted in Fig. 1.

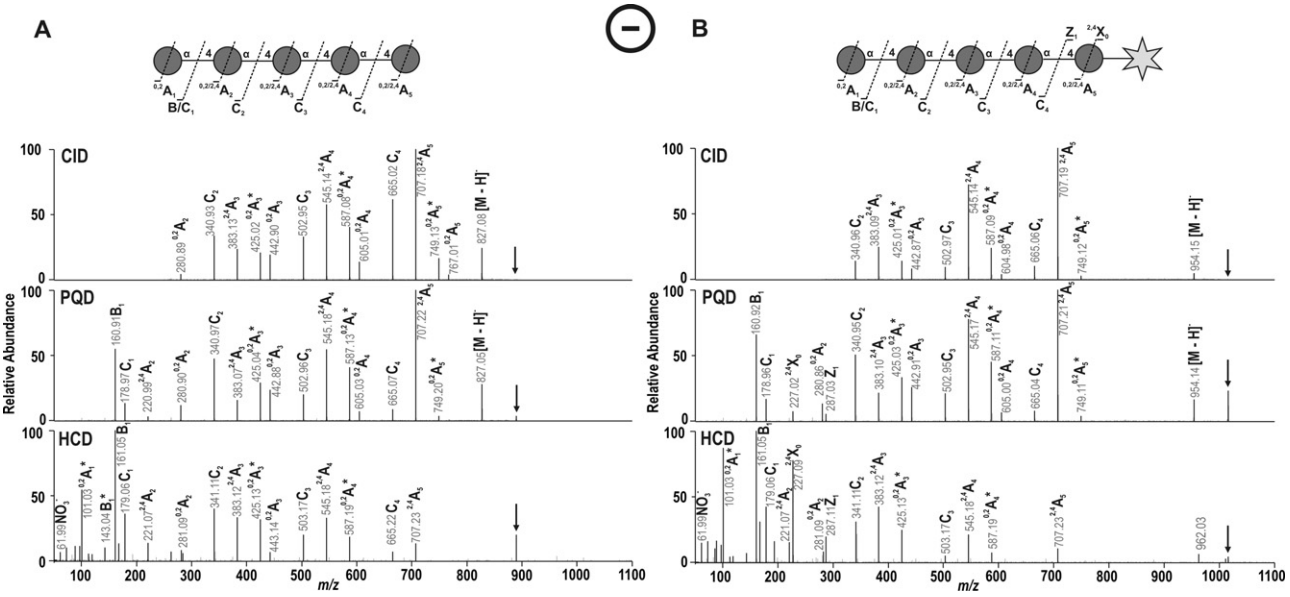

Fig. 3. Maltopentaose – spectra received by CID, PQD and HCD fragmentation with harmine (A)/3-AQ (B) in negative ion mode. Precursors are the respective adducts as depicted in Fig. 1.

Applying these three fragmentation techniques to maltopentaose in positive and negative ion modes yields spectra as illustrated in Figs. 2 and 3, respectively. Fragment ions are labeled according to the nomenclature proposed by Domon and Costello [22] (see Supplementary Data). Precursors are marked by arrows, and water losses are labeled with (*) following the respective fragments. Concerning the types of fragment ions observed, spectra are similar to those received by fragmentation using MALDI-TOF/TOF instruments. Using harmine as matrix for the underivatized molecule, positive ion mode MS/MS spectra are quite complex as fragmentation is not directed (see Fig. 2A). Depending on the localization of the sodium ion over the whole molecule, mostly C/Y- and B/Z-fragment ions or a combination of both is produced [15,16]. The symmetry of the molecule complicates peak assignment as fragment ions containing the reducing or the nonreducing end cannot be distinguished. Derivatization with 3-AQ generates protonated precursors whose fragmentation patterns are very simple (see Fig. 2B). Due to charge localization at the reducing end, promoting a directed fragmentation from the nonreducing end, the oligosaccharide's sequence can easily be determined. For a more detailed description of fragmentation patterns of 3-AQ-derivatized oligosaccharides see Rohmer et al. [28].

Using CID, the low-mass cut-off in the ion trap does not allow the detection of fragment ions below $m/z = 300$ for maltopentaose. Besides, CID spectra often show a harsh decrease in intensity towards lower mass fragment ions, resulting in poor sequence coverage. PQD fragmentation bypasses the "one-third rule" of CID. For all examined oligosaccharides, PQD proved to be of great value

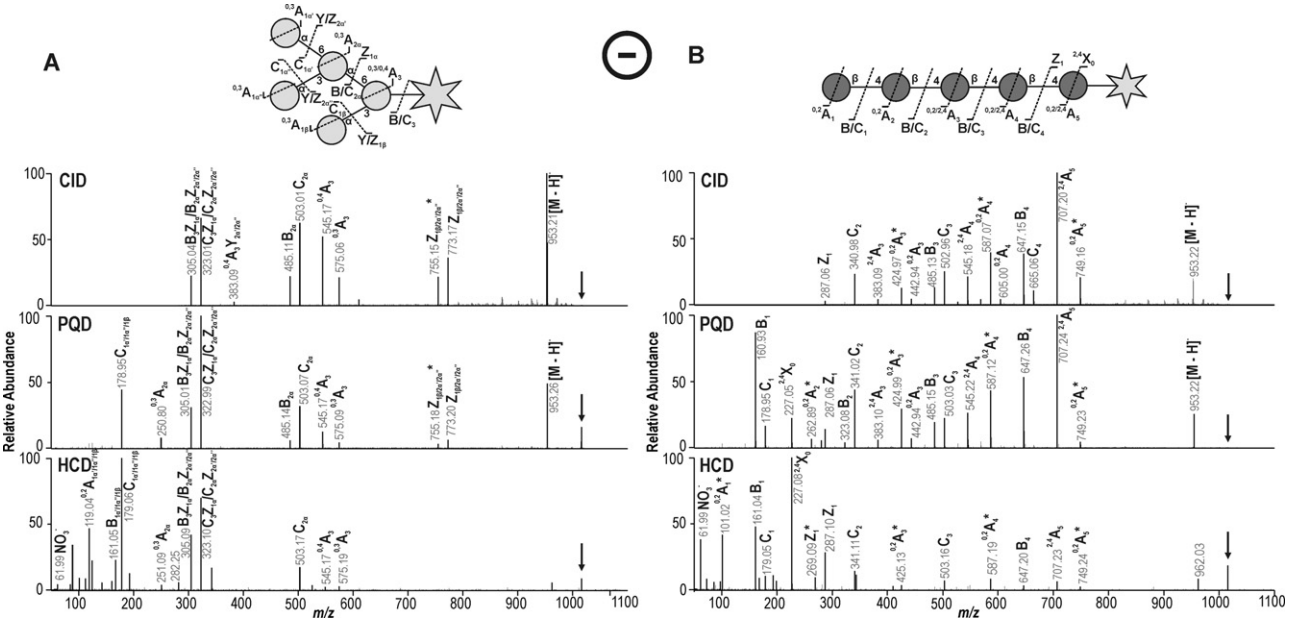

Fig. 4. 3α,6α-Mannopentaose (A) and cellopentaose (B) – CID, PQD and HCD spectra with 3-AQ in negative ion mode. Nitrate adducts of 3-AQ-derivatized species are chosen as precursors. Although only differing in α/β-configuration of glycosidic bonds, negative ion mode spectra of maltopentaose (Fig. 3B) and cellopentaose (B) show peaks with clearly different intensities.

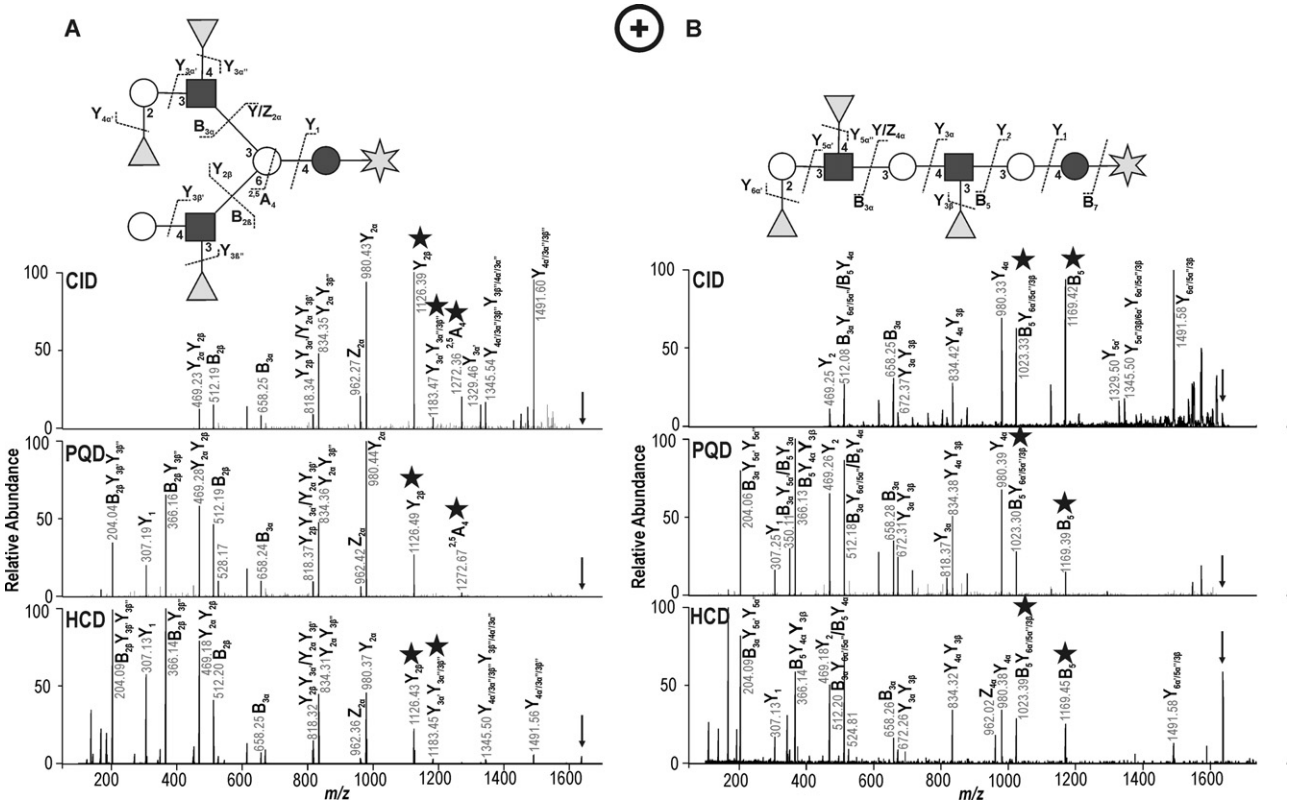

Fig. 5. TFLNH (A) and TFpLNH (B) – CID, PQD and HCD spectra with 3-AQ in positive ion mode. Protonated species were used as precursors. Fragments only appearing in the spectrum of one isomer are marked with black stars.

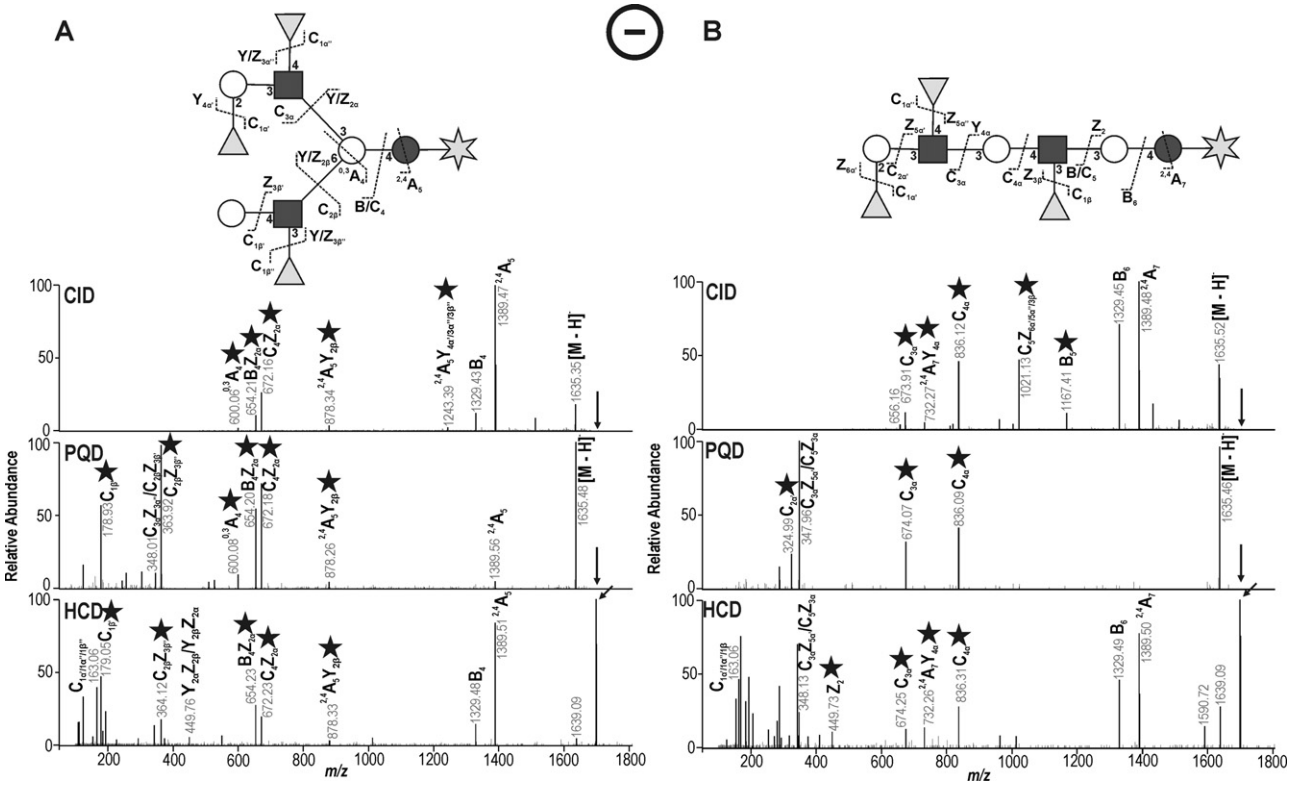

Fig. 6. TFLNH (A) and TFpLNH (B) – CID, PQD and HCD spectra with 3-AQ in negative ion mode. Nitrated species were used as precursors. Negative ion mode spectra of TFLNH and TFpLNH show even more distinct differences, as they provide information on linkage and branching. Fragments only appearing in the spectrum of one isomer are marked with black stars.

as ions covering the whole required m/z range are produced (see Figs. 2–6). However, the intensity of fragment ions is significantly lower (reduction by a factor of about 10) compared to CID, implying that the three-step process results in a loss of higher mass fragments. HCD fragmentation applies more energy to the precursors. The resulting spectra also reveal more low-mass fragment ions compared to CID, but do not reveal new fragment types. Moreover, HCD fragmentation exhibit comparably high detection limits, which is demonstrated in Section 3.4 of this article using a human milk oligosaccharide. Fragment ion detection in the low mass range was especially complicated due to electronic interfering signals. The intensity of resulting fragments is dependent on their successful transfer to the Orbitrap mass analyzer. This transfer is apparently not optimal, since the intensity of HCD fragment ions is significantly lower as those produced by CID (at least by a factor of 10). However, it has also been observed for CID and PQD that detection in the Orbitrap mass analyzer resulted in a loss of fragment ions. Therefore, if detection of HCD fragments was possible in the linear ion trap, spectra quality would possibly increase. Overall, detection in the Orbitrap mass analyzer should only be favored if high mass accuracy is needed. This is especially interesting for the analysis of complex human milk oligosaccharides, as they may contain structural elements differing only slightly in mass. For example, five fucose residues have almost the same mass as two *N*-acetyllactosamine subunits (Δm = 0.042 Da or 0.025 u monoisotopic mass) [44].

In negative ion mode, fragmentation of $[M+NO_3]^-$ ions of oligosaccharides preferentially starts at the reducing end, leading to consecutive C-type fragmentation following electron-pair rearrangement [13,23,34,45]. In most cases, MS/MS spectra are more structurally informative in negative ion mode compared to positive ion mode as cross-ring cleavages are more prominent. Those are essential for the characterization of an oligosaccharide's linkage and branching. Negative ion mode fragmentation of oligosaccharides has been mostly performed with ESI instruments [13,23,45,46] since $[M+NO_3]^-$ ions, exhibiting the lowest detection limits and good fragmentation behavior, only yield informative MS/MS spectra with ESI. Using MALDI-PSD, those adducts just lose the attached anion (e.g. NO_3^-) upon fragmentation, so that the neutral oligosaccharide remains [47] and that resulting MS/MS spectra are uninformative. Therefore, MALDI MS/MS spectra had to be acquired from less stable and thus less intense anionic adducts, e.g. $[M+Cl]^-$ ions of oligosaccharides [47–49]. In contrast to that, fragmentation of $[M+NO_3]^-$ ions is possible using the MALDI LTQ Orbitrap. This is possibly due to the completely different composition compared to other MALDI instruments. The use of a collision cell for fragmentation eliminates the need for rapid acceleration and deceleration of the analytes observed in TOF/TOF-instruments. The ability to fragment $[M+NO_3]^-$ ions of oligosaccharides using ESI-CID has already been demonstrated [13]. MALDI-Q-TOF fragmentation of anionic adducts of oligosaccharides has not been published up to this date, so that the issue whether the ion source or the mass analyzer is determining for the process has not been addressed. To sum up, the exact reason for the different fragmentation of $[M+NO_3]^-$ ions of oligosaccharides in the MALDI LTQ Orbitrap is unknown and should be examined in more detail at another point. By elimination of HNO_3, $[M-H]^-$ ions of oligosaccharides are produced, promoting the oligosaccharide's fragmentation from the reducing end. This presents a great advantage in MALDI analysis of oligosaccharides, as negative ion mode fragmentation can now be performed with a stable and intense oligosaccharide adduct. Resulting spectra are depicted in Fig. 3A and B for maltopentaose with harmine and 3-AQ, respectively. As already described for MALDI-PSD, negative ion mode fragmentation of 3-AQ-derivatized oligosaccharides does not differ significantly from that of underivatized oligosaccharides [28]. As demonstrated in Fig. 3, this also applies to the MALDI LTQ Orbitrap. Differences between CID, PQD and HCD spectra are generally the same as observed in positive ion mode. CID suffers from its low-mass cut-off, but fragments show the highest intensity. PQD yields fragments covering a wide m/z range, but fragment intensity is comparatively low. HCD spectra exhibit some additional fragments generated by the application of more energy in the lower mass range.

3.3. Differentiation of isomeric structures

3α,6α-Mannopentaose and cellopentaose were chosen for further experiments to demonstrate the ability of the MALDI LTQ Orbitrap analysis of 3-AQ-derivatized oligosaccharides to differentiate between oligosaccharides with different linkage positions, branchings and anomeric configurations of glycosidic bonds. 3-AQ was used as matrix and derivatizing agent for all further experiments, as resulting spectra gave precursors and fragments with intensities superior to harmine. 3α,6α-Mannopentaose is a commercially available structural element of high-mannose N-glycans. As displayed in Fig. 4A, it consists of five mannose residues linked to each other via α-1,3- and α-1,6-glycosidic bonds. Cellopentaose consists of five glucose monomers like maltopentaose, but exhibits β-1,4-linkages (for structures see Fig. 4). Both 3α,6α-mannopentaose and cellopentaose are isomeric to maltopentaose. Discrimination of linkage and anomeric configurations of glycosidic bonds is facilitated by fragmentation in negative ion mode due to more prominent cross-ring cleavages. Therefore, CID, PQD and HCD spectra of 3-AQ-derivatized $[M+NO_3]^-$ ions of 3α,6α-mannopentaose and cellopentaose were acquired (see Fig. 4). Resulting spectra follow the same trends as observed for maltopentaose. PQD spectra show a good intensity distribution over the whole m/z range, while HCD fragment ions are mainly found in the lower mass range. The identification of the individual isomer is possible as negative ion mode fragmentation produces characteristic fragment ions. Spectra of both 1,4-linked pentasaccharides (maltopentaose and cellopentaose, see Figs. 3B and 4A) Exhibit ^{2,4}A- and ^{0,2}A-fragment ions specific for this linkage [46]. Corresponding C-fragment ions are also quite prominent. In contrast to that, negative ion mode MS/MS spectra of 3α,6α-mannopentaose (as illustrated in Fig. 4B) are dominated by ^{0,3}A-, ^{0,4}A- and CZ-cleavages, indicating 1,3-substituted residues. Differences between maltopentaose and cellopentaose are more subtle, but yet well defined. One previously described method for the discrimination of anomeric configurations of 1,4-linkages relies on the relative intensities of cross-ring fragment ions $^{0,2}A^*$ (m/z = 263) and ^{0,2}A (m/z = 281) [25]. The ratio of 263/281 is said to be smaller than one for α-linkages and greater than one for β-linkages. This has only been verified for disaccharides and is difficult to apply to larger oligosaccharides since the important ions exhibit low intensities. Maltopentaose and cellopentaose spectra each display only one of the mentioned ions (^{0,2}A for maltopentaose and $^{0,2}A^*$ for cellopentaose), but these are consistent with the described rules. Here, a distinction based on these ions cannot be performed without PQD or HCD fragmentation. However, Figs. 3 and 4 show that B-ions (except for B_1) are not present in the spectrum of maltopentaose, but are very prominent for cellopentaose. If this theory was corroborated by different structures, it would clearly facilitate the assignment of anomeric configuration. The difference in the intensities of B- and C-ions has already been claimed for ESI-CID fragmentation of the identical structures [5] and infrared laser desorption of the respective trisaccharides [11] in positive ion mode. Negative ion mode MALDI-PSD spectra of maltohexaose and cellohexaose show the same difference, but this has unfortunately not been stated by the authors [47]. Instead of that, they claim that the difference between α- and β-glycosidic bonds is detectable via the relative intensities of ^{2,4}A- to $^{0,2}A^*$-ions (with the ratio of ^{2,4}A/$^{0,2}A^*$ being

much greater for α-glycosidic bonds). This is, except for the A_5 ions of cellopentaose with PQD, true for all glycosidic linkages in this experiment. Certainly, more isomeric structures have to be studied to prove this approach, but taking all information into account it is demonstrated that determination of glycosidic linkage type and even anomeric configuration is possible using Orbitrap fragmentation of $[M+NO_3]^-$ ions of 3-AQ-derivatized oligosaccharides.

3.4. Application to human milk oligosaccharides (HMOS)

In the following, the different fragmentation techniques are used to investigate trifucosyllacto-*N*-hexaose (TFLNH) and trifucosyl-para-lacto-*N*-hexaose (TFpLNH). TFLNH and TFpLNH are isomeric multiply fucosylated oligosaccharides occurring in human milk samples which structurally differ in only one single linkage. Therefore, TFLNH is branched, while TFpLNH has a linear core. Fig. 5 shows the structures of the 3-AQ-derivatized oligosaccharides and their CID, PQD and HCD spectra in positive ion mode. MALDI-TOF/TOF fragmentation of both isomers in positive and negative ion modes has already been discussed extensively [28]. Briefly, the isomers can be easily distinguished by fragmentation as intense peaks arise which appear in only one isomer's spectrum. Positive ion mode MS/MS spectra basically consist of B- and Y-ions. MALDI-Orbitrap fragmentation of HMOS in positive ion mode exhibits exactly the same fragments as already observed for MALDI-TOF/TOF fragmentation [28], but only using PQD and HCD fragmentation, the mass range below $m/z = 460$ is covered. Combining the information from CID, PQD and HCD spectra of the protonated 3-AQ-derivatized oligosaccharides, the whole mass range is covered and the complete sequence of both structures is elucidated (see Fig. 5). Although the additional fragments compared to CID spectra alone do not allow a better distinction of the isomers in this case, they add confidence to the assignment of the overall HMOS structure (e.g. $B_{2\beta}Y_{3\beta''}/B_5Y_{4\alpha}Y_{3\beta}$ is one *N*-acetyl-lactosamine unit). In positive ion mode, the branched isomer preferentially yields fragments resulting from cleavages at the branching points. As linkages at the reducing end of *N*-acetylhexosamine moieties are more labile and protonation is now also possible at their nitrogen atoms, positive ion mode spectra of 3-AQ-derivatized HMOS also include B-ions produced by cleavage next to those monomers. Besides the loss of respectively one and two fucoses, the $Y_{2\alpha}$ and $Y_{2\beta}$ fragment ions as well as the $^{2,5}A_4$ cross-ring fragment ion are detected with high abundance. Two of them, the $Y_{2\beta}$ and the $^{2,5}A_4$-fragment ions, can only be explained by the branched structure. The cross-ring fragment ion indicates a branching at positions 3 and 6. In contrast to fragmentation of underivatized fucose-containing oligosaccharides, only fucose residues at branching points are cleaved. The remaining fragments still contain all originally attached fucoses, so that their original position in the oligosaccharide molecule can easily be determined. To sum up, a distinction of the isomers is unproblematic. Black stars in the MS/MS spectra mark peaks only appearing in the spectrum of one structure.

In contrast to PSD fragmentation, where less stable $[M+Cl]^-$ ions have to be used for fragmentation, the MALDI LTQ Orbitrap enables fragmentation of $[M+NO_3]^-$ precursors. CID, PQD and HCD spectra of $[M+NO_3]^-$ ions of 3-AQ-derivatized TFLNH and TFpLNH are displayed in Fig. 6. Like in positive ion mode, characteristic peaks arising for each isomer are designated by black stars. MALDI-Orbitrap fragmentation of HMOS in negative ion mode also clearly resembles MALDI-TOF/TOF fragmentation [28]. However, additional cross-ring fragments are observed ($^{2,4}A_5Y_{4\alpha'/3\alpha''/3\beta''}$ and $^{2,4}A_5Y_{2\beta}$ for TFLNH, $^{2,4}A_7Y_{4\alpha}$ for TFpLNH), adding confidence to the assignment of 1,4-linkages. The big gap in the spectrum of TFLNH indicates the branched structure of the molecule. Our previous publication includes a more detailed description of the fragmentation pathway [28]. Taking the information from CID, PQD and HCD spectra together, coverage of the m/z range is improved. In negative ion mode, distinction of the two HMOS isomers is facilitated by PQD or HCD fragmentation, as unique fragments are detected for each isomer. $C_{1\beta'}$ at $m/z = 179$ is only present in TFLNH spectra, verifying its branched structure with an unsubstituted galactose residue at the nonreducing end [28]. $C_{2\beta}Z_{3\beta''}$ ($m/z = 364$) is characteristic for a 3-substituted GlcNAc residue with an unsubstituted Gal residue in position 4, which makes the distinction of lacto-series and lacto-*neo*-series possible. $C_{2\alpha'}$ ($m/z = 325$) is unique for TFpLNH, although not only explainable by its structure. Although yielding spectra with good mass range coverage, HCD fragmentation was impeded by electronic interfering signals and low detection limits, as described for maltopentaose. In order to illustrate this, a figure showing a series of HCD spectra in positive ion mode with decreasing amounts of 3-AQ-derivatized TFLNH was included in Supplementary Data. With 1 μl of oligosaccharide solution (0.1 mg/mL) spotted on the MALDI target, the total oligosaccharide amount used for the first spectrum is approximately 67 pmol. This yields HCD spectra with a total ion intensity of 8×10^5 a.u. When diluting the oligosaccharide solution 1:1 with water, the resulting HCD spectrum loses fragment ion intensity, and electronic interfering signals arise. This hinders fragment detection especially in the low mass range. When collision energy is increased in order to lift these low-mass fragments, the higher mass fragments disappear, while the interfering signals are still well visible. When the analyte solution is again diluted by 1:1, no more oligosaccharide fragments are detected. This means that the limit for an informative fragmentation of oligosaccharides with HCD is approximately 33 pmol, which is a significantly higher amount than those needed for CID or PQD fragmentation (approximately 5 or 16 pmol, respectively). Despite this low sensitivity, HCD fragmentation seems to be valuable for human milk oligosaccharides as HCD spectra exhibit a broader distribution of peaks over the whole mass range than observed with PQD. Additionally, some cross-ring fragments show high intensities in negative ion mode with HCD, which could be explained by the increased collision energy (see Fig. 6). This shows that although HCD fragmentation is quite problematic due to precursor isolation difficulties, it should not be completely disregarded. Different structures might yield different fragmentation patterns, and therefore, fragmentation with all three techniques might prove useful for structural elucidation. For HMOS, it is demonstrated that PQD and HCD fragmentation yield additional structural information since resulting spectra contain unique fragment ions of both isomers. Although giving very similar spectra compared to MALDI-TOF/TOF-fragmentation [28], MALDI LTQ Orbitrap fragmentation of oligosaccharides produces some additional cross-ring fragments which may increase structural information. Most notably, fragmentation in positive as well as negative ion mode should be carried out, as only both modes together yield complete information on sequence, linkage, branching and anomeric configuration of glycosidic bonds of oligosaccharides.

3.5. CID, PQD and HCD fragmentation: automation and post-processing

If all three fragmentation techniques should be used to increase informational gain by the fragmentation of oligosaccharides, a rapid and simple post-processing procedure is required. Moreover, fragmentation should be automated in order to simplify measurement proceedings. Acquisition of spectra from all three fragmentation mechanisms can be easily automatized using the Xcalibur software (Thermo Fisher Scientific, Bremen). For that purpose, a data-dependent MS/MS run is created which automatically selects precursors (by intensities or by mass lists)

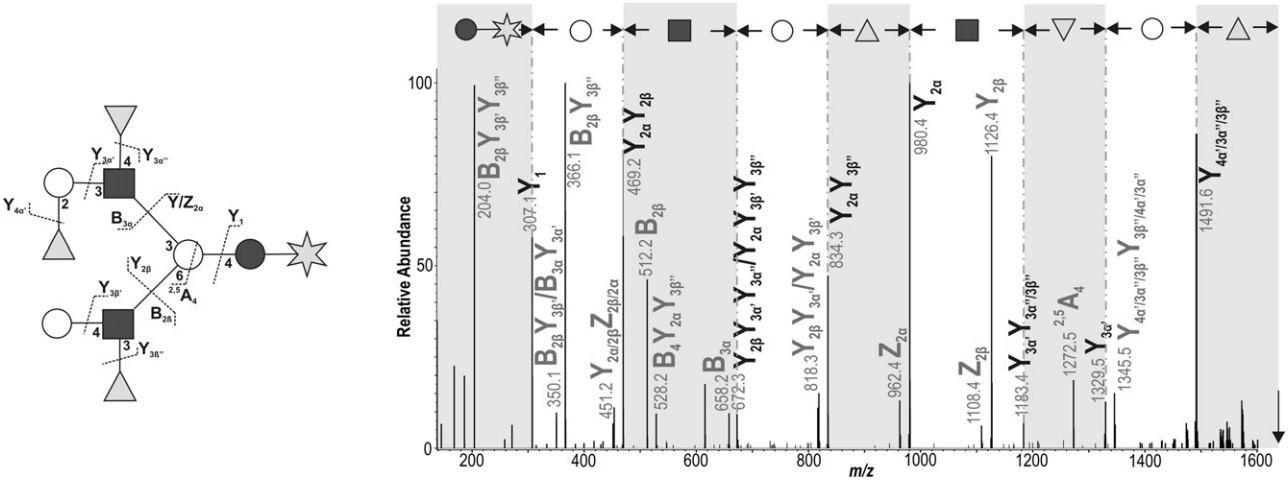

Fig. 7. TFLNH – spectrum obtained by combined peak lists of CID, PQD and HCD fragmentation in positive ion mode. A complete series of Y-ions is present, which is illustrated by white and grey bars defining the individual monosaccharides.

Table 2
TFLNH – GlycoWorkbench summary report for combined CID, PQD and HCD fragmentation in positive ion mode. The combination of peak lists leads to an extension of the fragment mass range, resulting in more complete information concerning the oligosaccharide's structure compared to CID fragmentation alone.

	Coverage[a]	RMSD[b]	Assigned	>10% assigned[c]	>5% assigned[d]
CID alone	68.21	0.0905	42/100 (42.00%)	13/18 (72.22%)	19/34 (55.88%)
CID + PQD + HCD	78.86	0.1056	105/208 (50.48%)	33/43 (76.74%)	51/74 (68.92%)

[a] Coverage is calculated by relating intensities of assigned peaks to those of total peaks.
[b] RMSD = root mean square deviation.
[c] Number of peaks with a relative intensity of more than 10% which could be assigned to theoretical fragment ions.
[d] Number of peaks with a relative intensity of more than 5% which could be assigned to theoretical fragment ions.

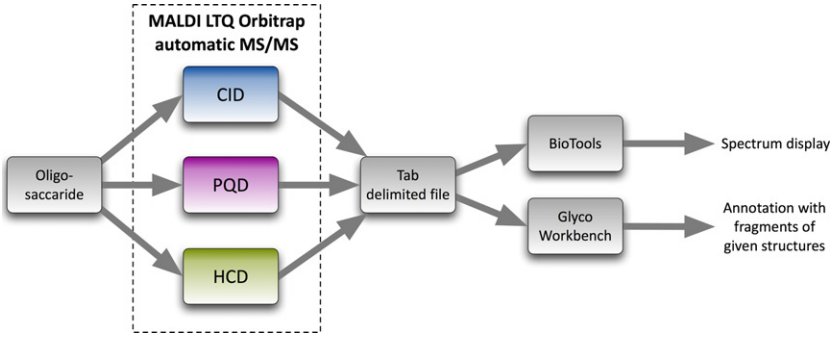

Fig. 8. Overall workflow: automation of CID, PQD and HCD fragmentation and post-processing of received peak lists.

and conducts fragmentation defined by a four-stage-experiment (single-MS + CID + PQD + HCD). In this setup, individual parameters can be adjusted for each fragmentation technique. Afterwards, multiple spectra generated by the same fragmentation technique can be displayed as one total spectrum in the QualBrowser for further analysis. This extremely facilitates Orbitrap measurements and allows a rapid evaluation of resulting spectra.

Subsequently, peak lists received by all three techniques were extracted by QualBrowser and combined into one single tab delimited file using relative peak intensities. Merged peak lists can be displayed and further processed in other programs, e.g. BioTools (Bruker Daltonics, Billerica, MA). As an example, the combined fragment spectrum for TFLNH in positive ion mode is displayed in Fig. 7. Fragments covering the whole m/z range are now present due to the combination of peak lists. Moreover, combined peak lists were forwarded to the GlycoWorkbench software for the determination of sequence coverage. There, these peak lists can be matched with theoretical fragments. The summary report created by GlycoWorkbench (see Table 2) gives information on sequence coverage (defined by intensities of assigned fragments divided by intensities of all fragments) and further statistical analysis. It is clearly visible that coverage and number of assigned peaks increases by using all three fragmentation techniques compared to CID alone. The overall workflow of automatic CID, PQD and HCD fragmentation and processing of combined peak lists is given in Fig. 8.

4. Conclusions

In this study, we examined the fragmentation behavior of underivatized as well as 3-AQ-derivatized oligosaccharides in the MALDI LTQ Orbitrap. The most striking advantage provided by the MALDI LTQ Orbitrap is the ability to fragment the stable and intense $[M+NO_3]^-$ ions of oligosaccharides in negative ion mode, promising a gain in sensitivity for oligosaccharide analysis. Fragmentation in positive and negative ion modes yielded complementary information. Combining all three fragmentation techniques provided by the Orbitrap (CID, PQD and HCD), fragment ions could be detected with high intensities over the whole m/z range.

To sum up, each fragmentation technique is, individually taken, not sufficient for complete structural characterization of oligosaccharides. The applied technique should be selected according to the m/z values of interesting fragments and the particular objective. If the whole mass range has to be considered, combining CID and PQD/HCD spectra is a possibility, like already demonstrated for iTRAQ quantitation of peptides [30,39,40]. Collecting all information received out of the three fragmentation techniques together with the use of both positive and negative ion modes makes full structural characterization of oligosaccharides reachable. The post-processing of spectra by a simple combination of peak lists via tab delimited files presents an easy possibility to enhance the information of fragment spectra of oligosaccharides. Moreover, automatic measurements make oligosaccharide analysis via Orbitrap fragmentation fast and reproducible.

Derivatization with 3-AQ led to improved detection limits and enhanced fragmentation behavior. In negative ion mode, a differentiation of isomeric standard oligosaccharides was possible due to distinct fragments concerning linkage, branching and anomeric configuration. The application of our approach to human milk oligosaccharides proves that this method is also able to differentiate between more complex isomers. Analysis of 3-AQ-derivatized *N*-glycans released from glycoproteins and of negatively charged oligosaccharides containing sialic acids or sulfate groups is currently under investigation and will be the subject of future publications. The combination of high mass accuracy and superior fragmentation possibilities using the MALDI LTQ Orbitrap and the convenient on-target derivatization with 3-AQ clearly facilitates oligosaccharide analysis.

Acknowledgements

We thank the Cluster of Excellence Macromolecular Complexes for their financial support.

Appendix A. Supplementary data

Supplementary data associated with this article can be found, in the online version, at doi:10.1016/j.ijms.2010.11.008.

References

[1] B. Stahl, M. Steup, M. Karas, F. Hillenkamp, Anal. Chem. 63 (1991) 1463.
[2] K.K. Mock, M. Davey, J.S. Cottrell, Biochem. Biophys. Res. Commun. 177 (1991) 644.
[3] B. Nilsson, Mol. Biotechnol. 2 (1994) 243.
[4] D.J. Harvey, J. Chromatogr. A 720 (1996) 429.
[5] U. Bahr, A. Pfenninger, M. Karas, B. Stahl, Anal. Chem. 69 (1997) 4530.
[6] D.J. Harvey, Mass Spectrom. Rev. 18 (1999) 349.
[7] J. Zaia, Mass Spectrom. Rev. 23 (2004) 161.
[8] D.J. Harvey, L. Royle, C.M. Radcliffe, P.M. Rudd, R.A. Dwek, Anal. Biochem. 376 (2008) 44.
[9] H. Lis, N. Sharon, Eur. J. Biochem. 218 (1993) 1.
[10] B. Spengler, J.W. Dolce, R.J. Cotter, Anal. Chem. 62 (1990) 1731.
[11] G.E. Hofmeister, Z. Zhou, J.A. Leary, J. Am. Chem. Soc. 113 (1991) 5964.
[12] D.J. Harvey, J. Am. Soc. Mass Spectrom. 11 (2000) 900.
[13] D.J. Harvey, J. Am. Soc. Mass Spectrom. 16 (2005) 622.
[14] J. Zaia, M.J.C. Miller, J.L. Seymour, C.E. Costello, J. Am. Soc. Mass Spectrom. 18 (2007) 952.
[15] B. Spengler, D. Kirsch, R. Kaufmann, J. Lemoine, Org. Mass Spectrom. 29 (1994) 782.
[16] D.J. Harvey, T.J. Naven, B. Küster, R.H. Bateman, M.R. Green, G. Critchley, Rapid Commun. Mass Spectrom. 9 (1995) 1556.
[17] D.J. Harvey, Int. J. Mass Spectrom. 226 (2003) 1.
[18] Y. Mechref, A.G. Baker, M.V. Novotny, Carbohydr. Res. 313 (1998) 145.
[19] Y. Mechref, P. Kang, M.V. Novotny, Rapid Commun. Mass Spectrom. 20 (2006) 1381.
[20] D.J. Harvey, R.H. Bateman, M.R. Green, J. Mass Spectrom. 32 (1997) 167.
[21] D.J. Harvey, R.H. Bateman, R.S. Bordoli, R. Tyldesley, Rapid Commun. Mass Spectrom. 14 (2000) 2135.
[22] B. Domon, C.E. Costello, Glycoconj. J. 5 (1988) 397.
[23] W. Chai, V. Piskarev, A.M. Lawson, Anal. Chem. 73 (2001) 651.
[24] W. Chai, A.M. Lawson, V. Piskarev, J. Am. Soc. Mass Spectrom. 13 (2002) 670.
[25] B. Guan, R.B. Cole, J. Am. Soc. Mass Spectrom. 19 (2008) 1119.
[26] F.N. Lamari, R. Kuhn, N.K. Karamanos, J. Chromatogr. B: Analyt. Technol. Biomed. Life Sci. 793 (2003) 15.
[27] T.J.P. Naven, D.J. Harvey, Rapid Commun. Mass Spectrom. 10 (1996) 829.
[28] M. Rohmer, B. Meyer, M. Mank, B. Stahl, U. Bahr, M. Karas, Anal. Chem. 82 (2010) 3719.
[29] J.C. Schwartz, J.E.P. Syka, S.T. Quarmby, The 53rd ASMS Conference on Mass Spectrometry and Allied Topics, TOD, 2005, p. 1135.
[30] T. Guo, C.S. Gan, H. Zhang, Y. Zhu, O.L. Kon, S.K. Sze, J. Proteome Res. 7 (2008) 4831.
[31] A. Kholomeev, A. Makarov, E. Denisov, O. Lange, W. Balschun, S. Horning, The 54th ASMS Conference on Mass Spectrometry and Allied Topics, TOB, 2006, p. 1035.
[32] J.V. Olsen, B. Macek, O. Lange, A. Makarov, S. Horning, M. Mann, Nat. Methods 4 (2007) 709.
[33] Q. Hu, R.J. Noll, H. Li, A. Makarov, M. Hardman, R.G. Cooks, J. Mass Spectrom. 40 (2005) 430.
[34] R.H. Perry, R.G. Cooks, R.J. Noll, Mass Spectrom. Rev. 27 (2008) 661.
[35] A. Makarov, E. Denisov, O. Lange, J. Am. Soc. Mass Spectrom. 20 (2009) 1391.
[36] K. Strupat, V. Kovtoun, H. Bui, R. Viner, G. Stafford, S. Horning, J. Am. Soc. Mass Spectrom. 20 (2009) 1451.
[37] A. Ceroni, K. Maass, H. Geyer, R. Geyer, A. Dell, S.M. Haslam, J. Proteome Res. 7 (2008) 1650.
[38] Y. Zhang, S.B. Ficarro, S. Li, J.A. Marto, J. Am. Soc. Mass Spectrom. 20 (2009) 1425.
[39] T. Köcher, P. Pichler, M. Schutzbier, C. Stingl, A. Kaul, N. Teucher, G. Hasenfuss, J.M. Penninger, K. Mechtler, J. Proteome Res. 8 (2009) 4743.
[40] L. Dayon, C. Pasquarello, C. Hoogland, J. Sanchez, A. Scherl, J. Proteomics 73 (2010) 769.
[41] N.E. Scott, B.L. Parker, A.M. Connolly, J. Paulech, A.V.G. Edwards, B. Crossett, L. Falconer, D. Kolarich, S.P. Djordjevic, P. Hojrup, N.H. Packer, M.R. Larsen, S.J. Cordwell, Mol. Cell Proteomics (2010), in press, doi:10.1074/mcp.M000031-MCP201.
[42] Z.M. Segu, Y. Mechref, Rapid Commun. Mass Spectrom. 24 (2010) 1217.
[43] J. Saba, S. Snovida, D. Charych, R. Viner, Thermo Scientific, App. Note 471 (2009).
[44] A. Pfenninger, S. Chan, M. Karas, B. Finke, B. Stahl, C.E. Costello, Int. J. Mass Spectrom. 278 (2008) 129.
[45] A. Pfenninger, M. Karas, B. Finke, B. Stahl, J. Am. Soc. Mass Spectrom. 13 (2002) 1331.
[46] A. Pfenninger, M. Karas, B. Finke, B. Stahl, J. Am. Soc. Mass Spectrom. 13 (2002) 1341.
[47] T. Yamagaki, H. Suzuki, K. Tachibana, Anal. Chem. 77 (2005) 1701.
[48] T. Yamagaki, H. Suzuki, K. Tachibana, J. Mass Spectrom. 41 (2006) 454.
[49] T. Yamagaki, H. Suzuki, K. Tachibana, J. Am. Soc. Mass Spectrom. 17 (2006) 67.